Journal of Physics and Chemistry of Solids 69 (2008) 2665–2669

Contents lists available at ScienceDirect

Journal of Physics and Chemistry of Solids

journal homepage: www.elsevier.com/locate/jpcs

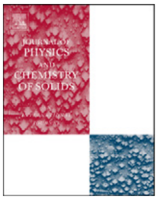

Versatile fabrication of dendritic cobalt microstructures using CTAB in high alkali media

Xian-Ming Liu [a], Wen-Liang Gao [b], Shao-Bin Miao [a], Bao-Ming Ji [a,*]

[a] College of Chemistry and Chemical Engineering, Luoyang Normal College, Luoyang 471022, PR China
[b] College of Chemistry and Chemical Engineering, Chongqing University, Chongqing 400044, PR China

ARTICLE INFO

Article history:
Received 27 January 2008
Received in revised form
10 May 2008
Accepted 17 May 2008

Keywords:
A. Magnetic materials
A. Metals
C. Electron microscopy
D. Microstructure

ABSTRACT

A facile hydrothermal reduction route based on a precipitate slow-release controlled process was developed to fabricate highly ordered dendritic cobalt microcrystals using cetyltrimethylammonium bromide (CTAB) in high alkali media. The shape, structure, and magnetic properties of the final products were investigated by X-ray diffraction (XRD), scanning electron microscopy (SEM), energy dispersive X-ray spectroscopy (EDS), transmission electron microscopy (TEM), electron diffraction (ED), and vibrating sample magnetometry (VSM). The results showed that the sample is hexagonal close-packed Co coexisting with cubic close-packed Co; the length of the main trunk is about 8 μm and diameter of the branches is 0.5–2 μm. Magnetic measurement at 300 K showed that these microstructures exhibited ferromagnetic character. The probable formation mechanism of the microcrystals was discussed on the basis of the experimental results.

1. Introduction

Magnetic materials have become the focus of intense research owing to their potential applications in high-density data storage, medical diagnosis, and bioseparation [1–5]. In most cases, the magnetic nanocrystals are superparamagnetic at room temperature because of their small dimensions and, thus, are not usable for many applications, such as magnetic recording. One way to increase the magnetic anisotropy of the particles is to modify their shape [6]. Another possible way to improve the magnetic anisotropy is to assemble nanocrystals into mutlidimensional morphologies [7–9].

Ferromagnetic cobalt has received considerable attention both theoretically and experimentally due to its extraordinary electrical, catalytic, and magnetic properties, which are of interest for basic scientific research and potential technological applications in, for example, high-density information storage, magnetic sensors, etc. [10–14]. It is well known that the properties of the products significantly depend on their morphologies and structures, so current research is focused on fabrication of ferromagnetic cobalt with specific morphologies and functions. In recent years, ferromagnetic cobalt with a wide range of morphologies such as wires [15,16], rods [7–9,17], disks [18], and rings [19,20] have been successfully synthesized. Various synthetic methods, including thermal decomposition of cobalt carbonyl [18,21,22] and organometallic precursors [7], template-mediated synthesis [23], solvothermal methods [24,25], and direct reduction method at room temperature [26], have also been proposed and demonstrated to prepare ferromagnetic cobalt. In addition to one-dimensional (1D) or two-dimensional (2D) assembled structures, some efforts have been focused on fabricating curved structures such as dendritic structures. Recently, Srivastava et al. [27] stated that bowl like cobalt was prepared by the infiltration of precursors in the interstitials of a colloidal template of polystyrene spheres. Imre and Balázs [28] synthesized tree like cobalt using an electrodeposition method. Hou et al. [29] synthesized uniform Co spherical assemblies by a facile hydrothermal reduction approach in the presence of surfactants of SDBS and found that the ordered spheres exhibit a high surface area and ferromagnetic character. Liu et al. [30] synthesized the highly ordered snowflake like metallic cobalt microcrystals via a hydrothermal reduction route in which it is easy to control the morphology and structure of snowflake like metallic cobalt nanocrystals by adjusting process parameters such as hydrothermal time and aqueous hydrazine concentration. Although the cobalt complex structures were synthesized by the above groups, design of a general method for the preparation of metal microstructures with a broad range of well-defined and controllable morphologies is still needed in order to fully exploit their peculiar properties and unique applications. In our previous work [31], we synthesized uniform Ni dendritic nanostructures by a facile hydrothermal reduction approach using cetyltrimethylammonium bromide (CTAB) as

---

[*] Corresponding author. Tel./fax: +86 379 65523821.
E-mail address: lliuxianming@yahoo.com.cn (B.-M. Ji).

0022-3697/$ - see front matter © 2008 Elsevier Ltd. All rights reserved.
doi:10.1016/j.jpcs.2008.05.023

surfactant in high basic media. It is significant to utilize this method to synthesize other ordered metallic dendritic structures, such as cobalt.

Herein we present the spontaneous, large-scale and hierarchical self-assembly of ordered cobalt microstructures. The ordered cobalt nanostructures were synthesized by hydrothermal reducing reaction in highly concentrated NaOH solution under mild conditions. In this synthetic system, soluble hydrated cobalt chloride was employed to supply a Co source, sodium hydroxide was used as a precipitator, aqueous hydrazine was used as a reducing agent, and CTAB was used as surfactant. These cobalt microstructures can be expected to bring new opportunities in vast research and application fields, such as sensors, microdevices, and magnetic cells.

2. Experimental

All reagents were analytic grade from Beijing Chemical Reagent Ltd. and were used without further purification. Cobalt microsized dendrites were synthesized by hydrothermal method at suitable temperatures. In a typical procedure, an aqueous solution of 35 mL was first prepared by dissolving $CoCl_2 \cdot 6H_2O$ (1.5 g) and CTAB (3.0 g) in deionized water. After adding 5 mL $N_2H_4 \cdot H_2O$ solution (v/v 80%) and 40 mL NaOH solution (20 mol/L) step by step into the above solution, the mixture was vigorously stirred for 10 min and then transferred into a teflon-lined stainless-steel autoclave with a capacity of 100 mL for hydrothermal treatment at 160 °C for 8 h. After the autoclave had cooled down to room temperature naturally, a black fluffy solid product was deposited at the bottom of the Teflon cup, indicating the formation of metallic Co. The final product was centrifuged, washed with deionized water and absolute ethanol several times to remove any alkaline salt and surfactants that remained in the final product, and then dried under vacuum at 40 °C for 48 h. The parameters that are essential for the special dendrite formation were studied by varying temperature, concentration of NaOH and the reaction time.

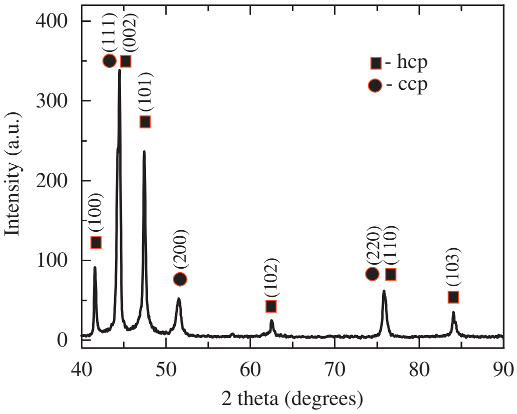

Fig. 1. XRD pattern of the sample prepared by hydrothermal method at 160 °C in 10 mol/L NaOH solution for 8 h.

XRD analysis was carried out on a Regaku D/max2500 diffractometer at a voltage of 40 kV and a current of 200 mA with Cu-Kα radiation ($\lambda = 1.5406$ Å), employing a scanning rate $0.02^\circ\,s^{-1}$ in the 2θ ranging from 5° to 90°. Transmission electron microscope (TEM) images and electron diffraction (ED) patterns were recorded on a Hitachi-600 TEM at an accelerating voltage of 200 kV. The scanning electron microscopy (SEM) images and electron dispersive X-ray spectrum (EDX) were obtained using a HITACHI S-4300 microscope and EMAX Horiba, respectively. Magnetic measurements were carried out at 300 K using a vibrating sample magnetometer (VSM, Lakeshore 7307, USA) with a maximum magnetic field of 10 kOe.

3. Results and discussion

Fig. 1 is the XRD pattern for the as-prepared Co sample synthesized via hydrothermal method in a high NaOH concentration solution system at 160 °C for 8 h. The peaks are assigned to diffraction from the (1 0 0), (0 0 2), (1 0 1), (1 0 2), (1 1 0) and (1 0 3) planes of hexagonal close-packed (hcp) Co, respectively, which are

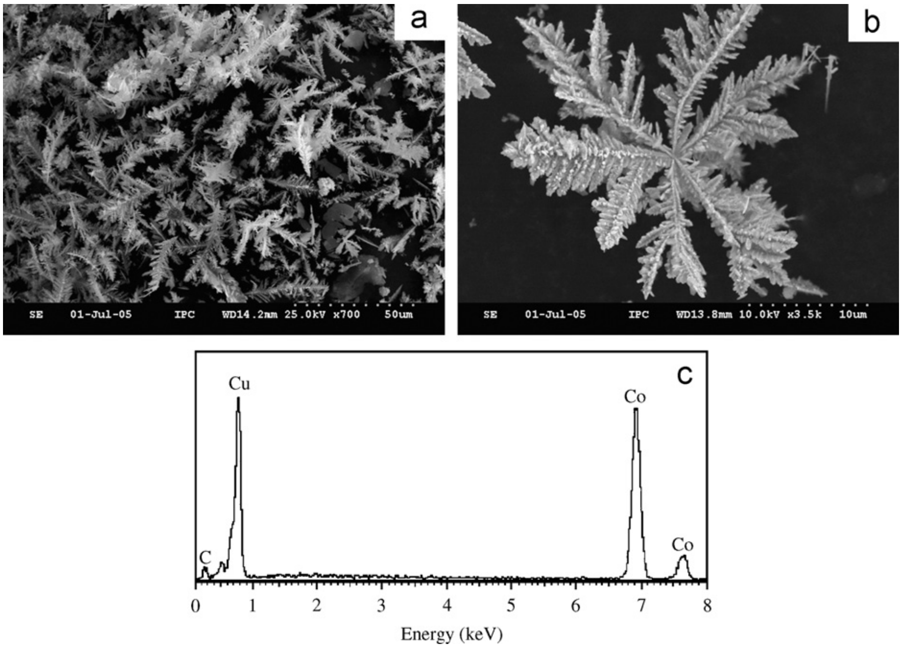

Fig. 2. SEM images of dendritic Co microstructures prepared by a hydrothermal reducing reaction. (a) Low magnification; (b) high magnification; (c) EDX spectrum of Co microstructures.

in agreement with the values in the JCPDS card (no. 05-0727). From the pattern, other characteristic peaks presenting cubic close-packed (ccp) Co have been observed, which indicates that both hcp and ccp phases of Co coexist in the sample. Generally, cobalt is stabilized in the hcp structure. The presence of ccp Co can be explained by the fact that the rapid growth of these structures causes considerable tensile stress. Though the hcp structure is the most stable phase for bulk Co at room temperature, ccp and hcp phases coexists in the same cobalt sample as relatively stable phases, as reported by Sun and Murray [32]. The ccp and hcp phases of cobalt are close-packed structures that differ only in the stacking sequence of atomic planes in the

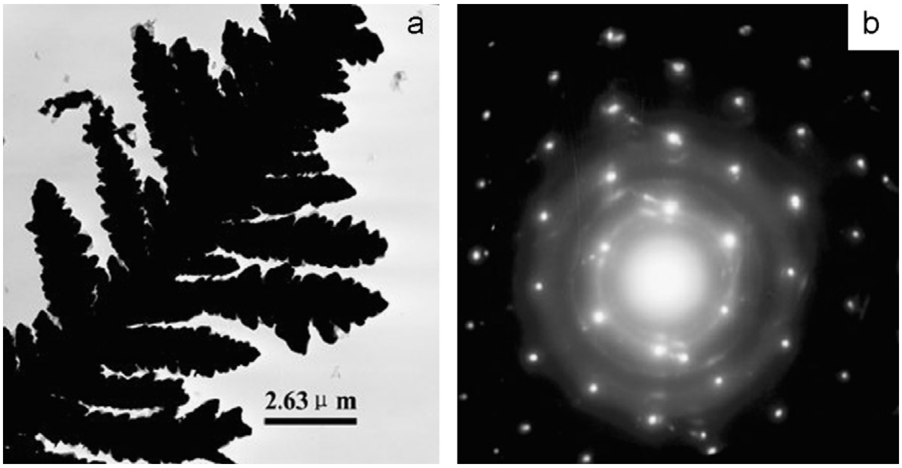

Fig. 3. TEM photograph (a) and ED pattern (b) of Co dendritic microstructures.

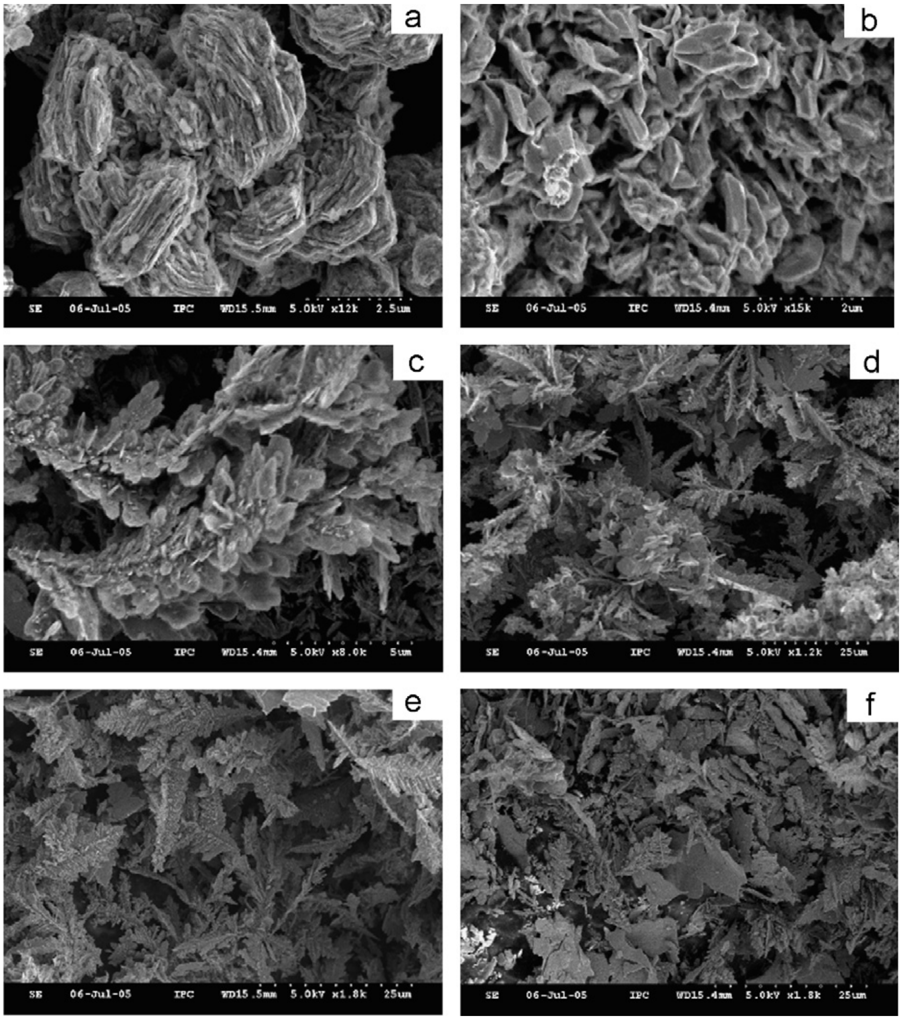

Fig. 4. SEM images of the samples prepared under different NaOH concentrations. (a) 2 mol/L; (b) 5 mol/L; (c) 15 mol/L; (d) 4 h; (e) 6 h; (f) 12 h.

cubic [1 1 1] direction. Low stacking faults energy could easily lead to the formation of both phases in the same sample.

Figs. 2a and b are the SEM images of the sample with different magnifications. The images show that the as-prepared samples are dendritic morphologies and most of the leaf like flakes exhibit radiating arrangement from the center. The uniformity of crystalline Co shows a good growth environment for Co dendrites. The chemical composition (atomic percent) is determined by EDX analysis under N_2 atmosphere. Fig. 2c shows a representative EDX spectrum of Co microstructures. In addition to the cobalt peaks, an oxygen and a carbon peak are also present; the low oxygen content may result from the Co surface oxidized by O_2 in the air because of high reaction activity of elementary Co, while the carbon content is ascribed to the conductive resin used to hold the sample.

The structure of the product was further examined with TEM and ED, as shown in Fig. 3. TEM image (Fig. 3a) demonstrates that the length of the main trunk is about 8 μm and diameters of the branches are 0.5–2 μm. The angles between the main trunk and side branches are close to 60°. ED pattern of an individual side branch reveals that it has two crystal structures with hcp and ccp phases. Furthermore, the ED patterns of the dendrite in different areas of an individual dendritic flake are almost the same. The ED pattern is matched with the XRD results.

The reduction mechanisms of Co element were described in detail in the literatures [26,30]. Before the hydrothermal treatment, soluble cobalt ions will first react with sodium hydroxide solution to form $Co(OH)_2$ precipitate, which can dissociate in water and form Co^{2+} slowly. Then $N_2H_4 \cdot H_2O$ can reduce Co^{2+} into metal Co via hydrothermal treatment.

The parameters that are essential for the special dendrite formation were studied by varying the hydrothermal temperature, the concentration of NaOH, the reaction time and CTAB, keeping other conditions unchanged. It can be seen from Figs. 4a–c that the concentration of NaOH has great influence on the formation of Co microstructures. When the concentration of NaOH is 2 or 5 mol/L, Co plate like structures are produced. While the concentration of NaOH increases to 15 mol/L, the morphology of the product is similar to dendritic structure, but the branches are plate like. It can be explained from the above results that NaOH concentration affects the reaction kinetics through tuning the dissolution–deposition equation of $Co(OH)_2$ and further affects the morphology of products. According to Peng's theory [33], the high chemical potential generated by a high monomer concentration in the growth solution favors grown along a certain direction. However, the higher NaOH concentration does not favor the formation of Co dendritic structures but prefers plate like structures. It is possible that the increase of the reactant concentration causes the increase of solution viscosity and the decrease of Co nuclei, which results in the formation of plate like Co structures. We have also performed the experiments by changing hydrothermal temperature. However, the temperature does not show obvious effect on the morphology of the final products. (The SEM images are omitted.) Figs. 4(d–f) show Co dendrites prepared at different times, keeping other conditions unchanged. When the hydrothermal reaction time is 4 or 6 h, similar dendritic structures appeared (Figs. 4d and e), but the branch length is very short. It can be found that the microcrystal size increases with the increase of the reaction time. While the time elongates to 12 h, the dendritic structures together with platelike Co microcrystal were obtained. It can be concluded that the reaction time had great influence on the growth of Co dendritic microstructures.

To investigate the influence of the surfactant, comparision experiments without CTAB were performed. It can be observed from Fig. 5a that the platelike Co particles were formed, indicating that the use of CTAB played a role in forming the dendritic structures. As we know, CTAB as a cation surfactant can combine with the growth unit, i.e. $Co(OH)_2$, due to the action of coulomb force [34]. However, the capsule of CTAB cannot be formed in the aqueous solution at 200 °C, which is higher than 180 °C based on the previous report [35]. Therefore, CTAB can absorb on the surface of the growth unit as shown in Fig. 5b. Due to the hydrophobic group around the circumference of CTAB, the growth of cobalt is preferential. Finally, Co dendritic microstructures are obtained due to the direct reduction under hydrothermal treatment. Therefore, with a reduction of hydrazine in high basic solution, highly ordered Co microstructures can be produced under suitable conditions. High basic media can provide the special environment favorable for the nucleation and growth of

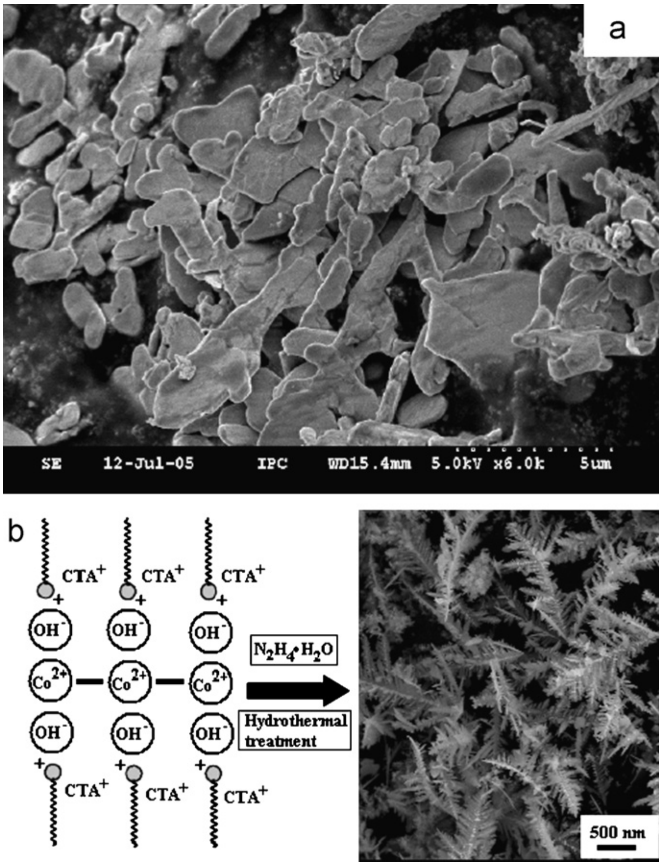

Fig. 5. (a) SEM image of the sample prepared without CTAB; (b) schematic drawing of the formation mechanism for the cobalt microstructures.

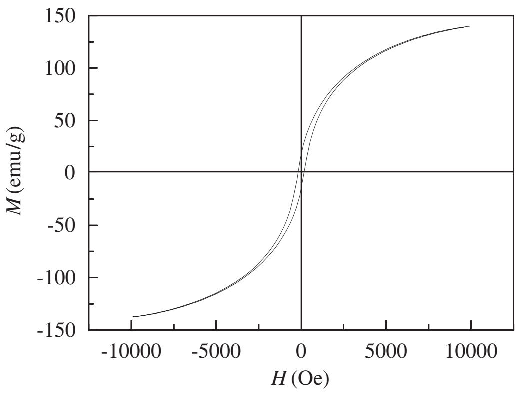

Fig. 6. Hysteresis loops of cobalt nanostructures at 300 K.

cobalt microcrystals with anisotropic morphologies. Meanwhile, the strong crystalline intrinsic anisotropy of hexagonal cobalt itself also influences the crystal structure and the final shape in the present synthetic route [21].

As well-known, the physical and chemical properties of functional materials strongly depend on the size, size distribution, defect structures, and dimensions. The magnetic properties were investigated by the magnetization dependence of applied fields at 300 K, as shown in Fig. 6. It can be observed that the sample shows hysteresis behavior, revealing that the Co microstructures are ferromagnetic. The saturation magnetization (M_s), remanent magnetization (M_r), and coercivity (H_c) for the sample are 138.6 emu/g, 16.2 emu/g and 175 Oe, respectively. All these are much lower than the corresponding values of the bulk cobalt ($M_s = 168$ emu/g, $H_c = 1500$ Oe), and the coercivity value of the sample is different from the coercivity of the reported data [30]. We thought that all the magnetic features different from the bulk Co and other Co particles may be attributed to their special shape. The present product has a relatively small coercivity, even though it consists of hcp Co microstructures with high shape anisotropy. This might be partly due to the multidomain structure and partly due to surface oxidation. Generally, the M_s for magnetic materials is lower than that for bulk material because the spin disorder on the surface and surface oxidation would significantly reduce the total magnetic moment. However, the magnetization hysteresis loop is symmetric with respect to the zero fields. This suggests that there is no exchange biasing effect caused by CoO, because the exchange coupling between ferromagnetic Co and the adjacent antiferromagnetic CoO would otherwise result in a shift of the hysteresis loop. It also indicates that the as-obtained Co microstructures have no significant oxidization.

4. Conclusions

In summary, we have successfully synthesized the highly ordered metallic cobalt dendritic structures via hydrothermal reduction method. The experimental results demonstrated that it is possible to control the morphology and structure of metallic cobalt crystals by adjusting process parameters such as NaOH concentration. The shape, structure and magnetic properties of the final products were investigated, and the formation mechanism of metallic cobalt microstructures was also discussed. The ordered microstructures exhibited ferromagnetic character. The material can be expected to have promising applications for catalysts and other related devices.

Acknowledgments

We appreciate the financial support of the Henan Innovation Project for University Research Talents (No. 2005KYCX021).

References

[1] S. Sun, C.B. Murray, D. Weller, L. Folksv, A. Moser, Science 287 (2000) 1989.
[2] Y. Hou, H. Kondoh, T. Kogure, T. Ohta, Chem. Mater. 16 (2004) 5149.
[3] T. Hyeon, Chem. Commun. (2003) 927.
[4] D.L. Peng, T. Asai, N. Nozawa, T. Hihara, K. Sumiyama, Appl. Phys. Lett. 81 (2002) 4598.
[5] H.H. Yang, S.Q. Zhang, X.L. Chen, Z.X. Zhuang, J.G. Xu, X.R. Wang, Anal. Chem. 76 (2004) 1316.
[6] V.F. Puntes, K.M. Krishnan, A.P. Alivisatos, Science 291 (2001) 2115.
[7] F. Dumestre, B. Chaudret, C. Amiens, M. Respaud, P. Fejes, P. Renaud, P. Zurcher, Angew. Chem. Int. Ed. 42 (2003) 5213.
[8] M.P. Pileni, J. Phys. Chem. B 105 (2001) 3358.
[9] J. Legrand, A.T. Ngo, C. Petit, M.P. Pileni, Adv. Mater. 13 (2001) 58.
[10] C. Petit, A. Taleb, M.P. Pileni, Adv. Mater. 10 (1998) 259.
[11] C. Stamm, F. Marty, A. Vaterlaus, V. Weich, S. Egger, U. Maier, U. Ramsperger, H. Fuhrmann, D. Pescia, Science 282 (1998) 499.
[12] C. Petit, T. Cren, D. Roditchev, W. Sacks, J. Klein, M.P. Pileni, Adv. Mater. 11 (1999) 1198.
[13] J. Legrand, C. Petit, M.P. Pileni, J. Phys. Chem. B 105 (2001) 5643.
[14] P. Gambardella, S. Rusponi, M. Veronese, S.S. Dhesi, C. Grazioli, A. Dallmeyer, I. Cabria, R. Zeller, P.H. Dederichs, K. Kern, C. Carbone, H. Brune, Science 300 (2003) 1130.
[15] H.Q. Cao, Z.H. Xu, D. Sang, C.Y. Sheng, Adv. Mater. 13 (2001) 121.
[16] L. Vila, P.L. Vincent, D.-D. Pra, G. Pirio, E. Minoux, L. Gangloff, S.D. Champagne, N. Sarazin, E. Ferain, R. Legras, L. Piraux, P. Legagneux, Nano Lett. 4 (2004) 521.
[17] F. Dumestre, B. Chaudret, C. Amiens, M.C. Fromen, M.J. Casanove, P. Renaud, P. Zurcher, Angew. Chem. Int. Ed. 41 (2002) 4286.
[18] V.F. Puntes, D. Zanchet, C.K. Erdonmez, A.P. Alivisatos, J. Am. Chem. Soc. 124 (2002) 12874.
[19] S.L. Tripp, S.V. Pusztay, A.E. Ribbe, A. Wei, J. Am. Chem. Soc. 124 (2002) 7914.
[20] S.L. Tripp, R.E. Dunin-Borkowski, A. Wei, Angew. Chem. Int. Ed. 42 (2003) 5591.
[21] D.P. Dinega, M.G. Bawendi, Angew. Chem. Int. Ed. 38 (1999) 1788.
[22] V.F. Puntes, K.M. Krishnan, A.P. Alivisatos, Science 291 (2001) 2115.
[23] M. Knez, A.M. Bittner, F. Boes, C. Wege, H. Jeske, E. Mai, K. Kern, Nano Lett. 3 (2003) 1079.
[24] H.L. Niu, Q.W. Chen, H.F. Zhu, Y.S. Lin, X. Zhang, J. Mater. Chem. 13 (2003) 1803.
[25] Y. Zhu, Q. Yang, H. Zheng, W. Yu, Y. Qian, Mater. Chem. Phys. 91 (2005) 293.
[26] Y. Zhu, H. Zheng, Q. Yang, A. Pan, Z. Yang, Y. Qian, J. Cryst. Growth 260 (2004) 427.
[27] A.K. Srivastava, S. Madhavi, T.J. White, R.V. Ramanujan, J. Mater. Chem. 15 (2005) 4424.
[28] A.R. Imre, L. Balázs, Fractals 8 (2000) 349.
[29] Y. Hou, H. Kondoh, T. Ohta, Chem. Mater. 17 (2005) 3994.
[30] X. Liu, R. Yi, Y. Wang, G. Qiu, N. Zhang, X. Li, J. Phys. Chem. C 111 (2007) 163.
[31] X.M. Liu, S.Y. Fu, J. Cryst. Growth 306 (2007) 428.
[32] S. Sun, C.B. Murray, J. Appl. Phys. 85 (1999) 4325.
[33] Z.A. Peng, X.G. Peng, J. Am. Chem. Soc. 123 (2001) 1389.
[34] L. Gmelin, H. Watts, Hand-Book of Chemistry, Cavendish Society, London, 1980.
[35] M. Cao, C. Hu, G. Peng, Y. Qi, E. Wang, J. Am. Chem. Soc. 125 (2003) 4982.